University of Dundee

Alkoxy-functionalised dihydropyrimido[4,5-b]quinolinones enabling anti-proliferative and anti-invasive agents

Patel, Subham G.; Sharma, Ira; Parmar, Mehul P.; Nogales, Joaquina; Patel, Chirag D.; Bhalodiya, Savan S.

Document Version
Peer reviewed version

Link to publication in Discovery Research Portal

Alkoxy-Functionalised Dihydropyrimido[4,5-*b*]quinolinones enabling Anti-Proliferative and Anti-Invasive Agents

Subham G. Patel [a,c,1], Ira Sharma [b,1], Mehul P. Parmar [a], Joaquina Nogales [b], Chirag D. Patel [a], Savan S. Bhalodiya [a], Disha P. Vala [a], Niraj V. Shah [c], Sourav Banerjee [b*], and Hitendra M. Patel [a*]

[a] *Department of Chemistry, Sardar Patel University, Vallabh Vidyanagar, 388120, Gujarat, India*

[b] *Department of Cellular and Systems Medicine, School of Medicine, University of Dundee, Dundee, UK*

[c] *J & J College of Science, Nadiad – 387001, Kheda, Gujarat, India*

[1] *authors contributed equally*

* Co-corresponding Authors: Hitendra M. Patel, E-mail: *hm_patel@spuvvn.edu*.
Sourav Banerjee, E-mail: s.y.banerjee@dundee.ac.uk.

Abstract

We report the synthesis of a bioactive novel series of Alkoxy-functionalised Dihydropyrimido[4,5-*b*]quinolinone derivatives using a multicomponent microwave-assisted reaction scheme. Anti-glioma bioactivity was observed in specific molecules within the library of 20 derivatives. Out of the compounds, **5c** had the most potent anti-proliferative activity with half maximal effective concentration of less than 3 micromolar against primary patient-derived glioblastoma cells and was selected for further study. Compound **5c** effectively inhibited invasion and tumour growth of 3D primary glioma cultures in a basement membrane matrix. This suggests that the novel compounds could inhibit both the proliferation and invasive spread of glioma. Through our current work, we establish a promising series of Dihydropyrimido[4,5-*b*]quinolinone based lead compounds with anti-cancer activity.

Keywords: Microwave-assisted reaction, Multicomponent reaction, Pyrimido[4,5-*b*] quinolinone, Anti-proliferative, Anti-invasive agents

1. Introduction

The global burden of cancer is predicted to rise in the coming decades due to ageing population and urbanization.[1] Cancer is a disease in which one or more cells lose control of their growth, resulting in a solid mass of cells known as a tumor.[2] Malignant gliomas are the most common adult primary brain tumors and one of the most severe malignancies, with a median

survival time of 12 to 15 months[3]. It is one of the leading causes of death worldwide, and the most common treatments encompass surgery, chemotherapy, and/or radiotherapy.[4] Various interventional and therapeutic options are being pursued for gliomas and still it remains a major un-met need to this day[5-7]. With the rise in cancer incidence, the need for the development of cytotoxic drugs is increasing day by day in the modern era.
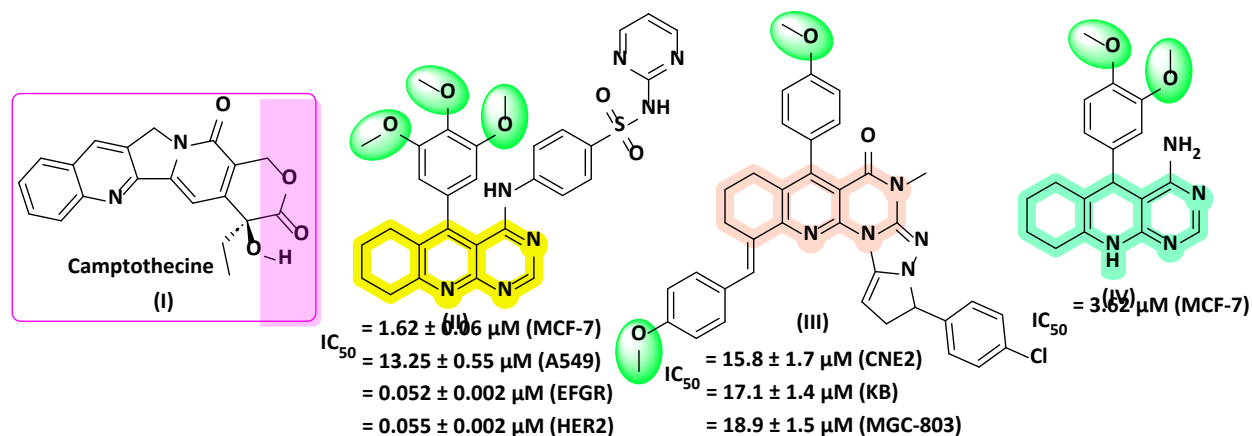
Figure 1 Potent anticancer agents

The strategic development of a chemical reaction route that maximizes structural complexity and diversity, while simultaneously reducing synthetic steps, poses a significant challenge in drug discovery.[8] Multicomponent reactions (MCRs) accelerated by Microwave irradiation (MWI) are a very powerful approach based on green chemistry aspects.[9] Microwave irradiation was discovered to be the most effective technique for activating chemical compounds, attributed to its capacity to expedite reaction times, augment conversion rates, and improve selectivity.[10] Microwave-assisted multicomponent reactions (MCRs) have emerged as a prominent and efficient synthetic methodology exploring the synthesis of biologically active compounds with diverse heterocyclic scaffolds.
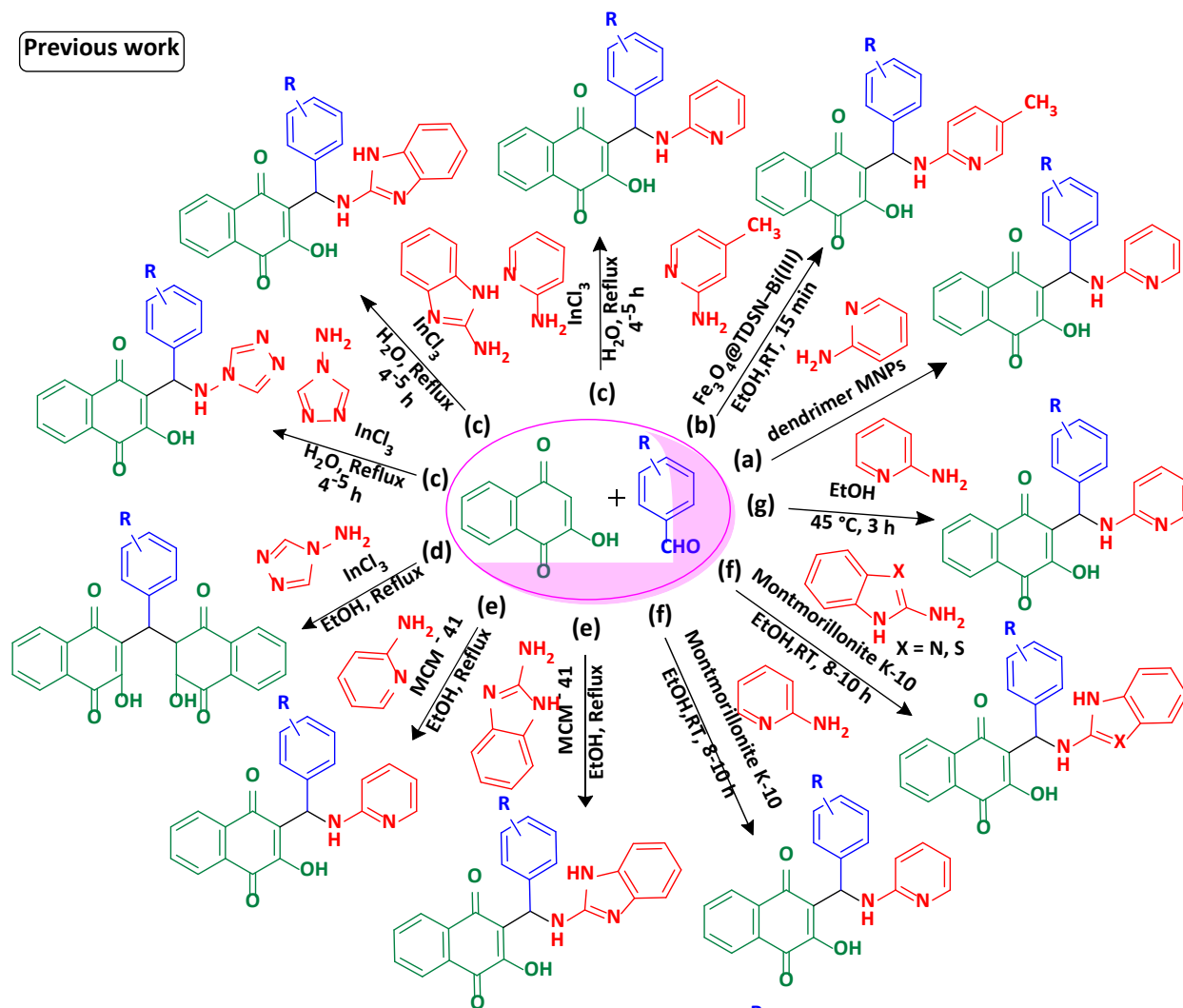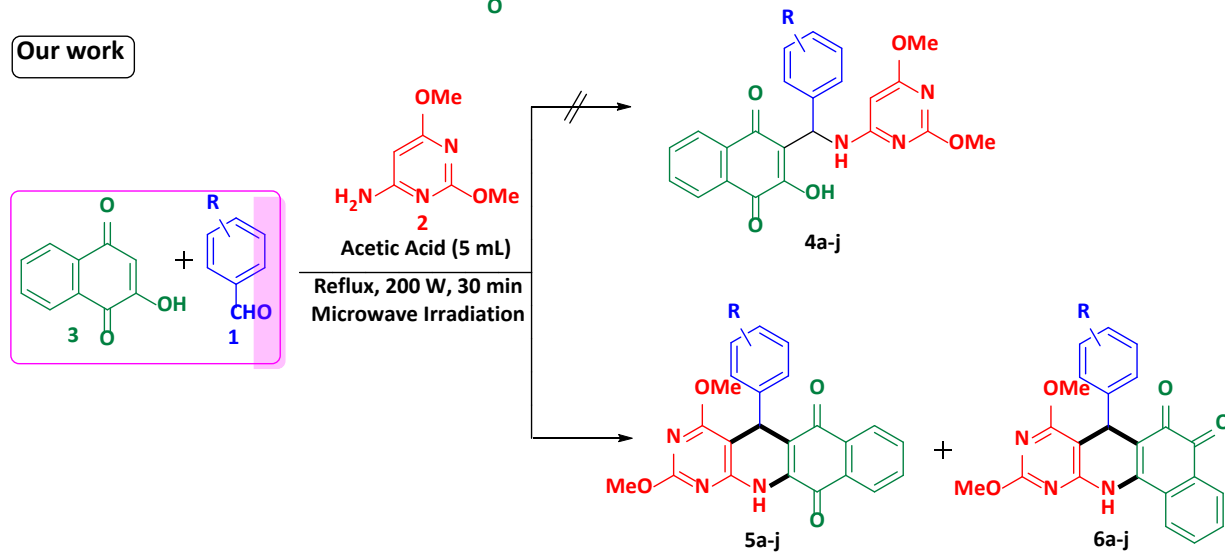
Scheme 1 Multicomponent reaction of aryl aldehyde, heteroaromatic amine and lawsone.

The quinoline core, inherent in numerous alkaloids, is associated with potent antitumor activity, as seen in the case of camptothecin **I**.[11] Empirical findings highlighting the potency of anticancer activity in a diverse range of quinolines and their derivatives.[12-15] Evidence from research underscores the importance of the pyrimido[4,5-*b*]quinolines (PQs) nucleus as a central pharmacophore in the development of anticancer therapeutics.[16-20] Scientific evidence suggests that methoxy group incorporation into heterocycles enhances their potential for antitumor or anticancer activity. Fig. 1 highlights the potent anticancer attributes of molecules **II, III** and **IV**, primarily attributed to the methoxy group-containing pyrimido[4,5-*b*]quinoline motif embedded in their molecular frameworks.[21-23] Several anticancer drugs such as bosutinib[24], brigatinib[25], cabazitaxel[26], erdafitinib[27], lurbinectedin[28], and trabectedin[29] are characterized by the presence of methoxy groups within their chemical frameworks.

The multicomponent reaction of heteroaromatic amine, lawsone (2-hydroxy-1,4-naphthoquinone) and aldehyde has been extensively studied by multiple research groups, employing various catalysts like Fe_3O_4@TDSN–Bi[30, 31], $InCl_3$[32, 33], MCM-41[34], Montmorillonite K-10[35], dendrimer MNPs γ-Fe_2O_3/SiO_2-propyl-NH-AMAM-SO_3H[36], and even under catalyst-free[37] conditions (Scheme 1). Aminonaphthoquinone derivatives emerged as notable products in these investigations. To the best of our knowledge, the current literature lacks alternative methodologies for the synthesis of dihydropyrimido[4,5-*b*]quinolines (DHPQs) through the utilization of heteroaromatic amine and lawsone. Hence, the exploration of novel and diverse strategies for their acquisition remains imperative, given their inherent significance.

Drawing inspiration from the findings of these studies and our ongoing research endeavours to synthesise new bioactive heterocycles via multicomponent synthesis[38-43], we first time report acetic acid catalysed green and efficient protocol for the synthesis of methoxy conjugated DHPQs. We produce these DHPQs via microwave assisted multicomponent rection of methoxy aldehyde, 6-amino-2,4-dimethoxypyrimidine, and lawsone (Scheme 1).

2. Results and discussions

2.1 Chemistry

Our initial examination began with the multicomponent reaction of *p*-methoxybenzaldehyde **1a**, 6-amino-2,4-dimethoxypyrimidine **2**, and lawsone **3** in equimolar ratio to achieve our targeted **4a**. we made our first attempt to synthesize the desired DHPQ under solvent-free conditions resulted in formation sticky mass with no observable conversion of **1a** (Table 1, entry 1). Subsequently, we introduced water as a solvent, encountering challenges with incomplete conversion of **1a** (Table 1, entry 2). Following this initial phase, our reaction was systematically screened with various solvents such as ethanol, methanol, acetonitrile, DMF, acetic acid, and ethyl L-lactate under reflux conditions (Table 1, entry 3-8). Optimal outcomes

were achieved when glacial acetic acid served as the solvent in 1.5 h (Table 1, entry 5). In the course of this experiment, the formation of the product was observed within the reaction medium under reflux conditions.

Table 1. Optimization of solvent for the reaction.[a]

Entry	Solvent [b]	Temperature	Time	Conversion relative to aldehyde [c]
1	Solvent-free	100 °C	12 h	NR
2	Water	reflux	12 h	Incomplete
3	Ethanol	reflux	6 h	100 %
4	Methanol	reflux	8 h	100 %
5	**Acetic acid**	**reflux**	**1.5 h**	**100 %**
6	Ethyl L-lactate	reflux	3 h	100 %
7	Acetonitrile	reflux	6 h	Incomplete
8	DMF	reflux	4 h	Incomplete

[a] Reaction condition: 1 mmol *p*-methoxybenzaldehyde **1a**, 1 mmol 6-amino-2,4-dimethoxypyrimidine **2** and 1 mmol lawsone **3,** reflux

[b] 5 mL solvent

[c] Observed from TLC analysis

Thin-layer chromatographic (TLC) observations signify the complete conversion of **1a** (Table 1, entry 3-6), accompanied by the appearance of two distinct spots with differing polarities on the TLC plate. The crude product was isolated and subsequently characterized through liquid chromatography-mass spectrometry (LCMS) analysis, revealing the existence of two molecular ion peaks with equivalent molar masses, distinct from our targeted product **4a**. For identification of the product, we conducted the separation the crude product using flash chromatography, with mobile phase consisting of 50% ethyl acetate and 50% n-hexane. Upon completion of the separation, the specific fraction of the molecule was introduced into the rotary evaporator, initiating the evaporation of solvent under reduced pressure while keeping the temperature within the 60 – 70°C, resulting in the isolation of the pure product.

Structural elucidation via ^{1}H-NMR did not align with the expected structure **4a**, pointing towards the formation of compounds **5a** and **6a** (see Scheme 1), accompanied by the establishment of a newly formed ring structure. As a matter of fact, the positioning of two carbonyl groups in an ortho arrangement within a naphthoquinone ring results in a considerable downfield shift in their signals. Furthermore, the extremely close proximity of the two-carbonyl resonance at 180.51 and 179.06 ppm, signifying highly adjacent chemical shifts for the carbonyl

^{13}C-NMR signals, strongly suggests the presence of an orthoquinone moiety, as depicted in the structure of **6a**.

Table 2 Optimization of time and microwave irradiation power for the reaction.[a]
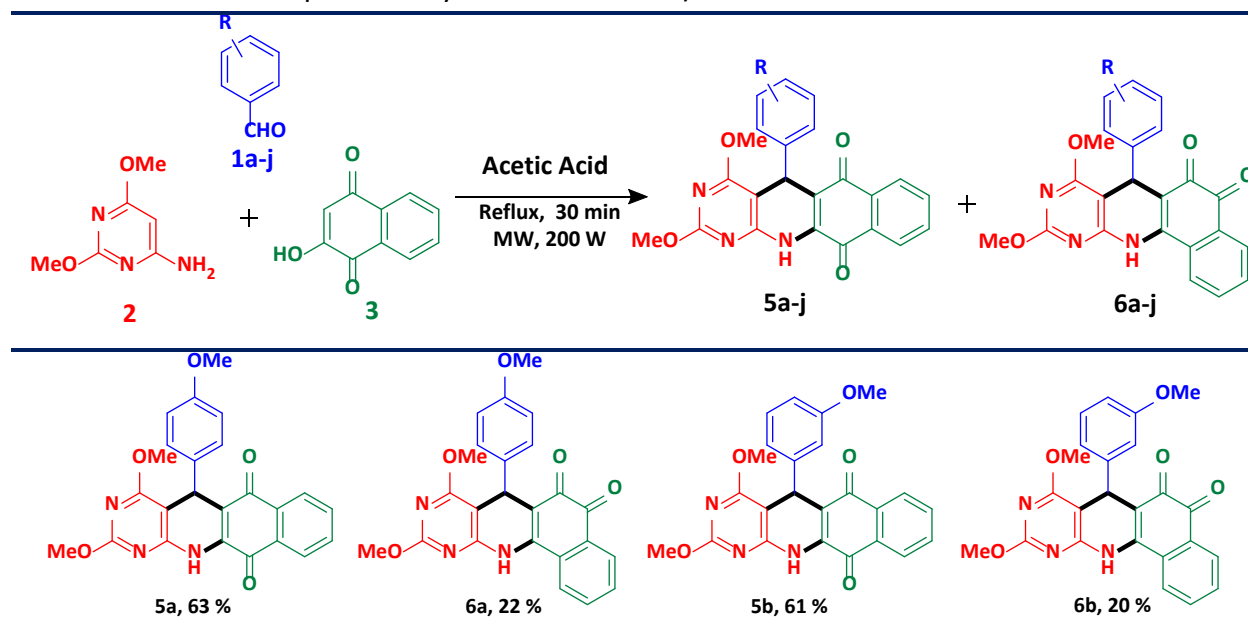
Entry	Power (w)	Time (min)	Yield [23] [b]
1	300	45	88
2	250	40	91
3	200	40	94
4	**200**	**30**	**94**
5	150	45	86

[a] Reaction condition: 1 mmol *p*-methoxybenzaldehyde **1a**, 1 mmol 6-amino-2,4-dimethoxypyrimidine **2** and 1 mmol lawsone **3,** reflux, 5 mL glacial acetic acid, reflux

[b] Crude product yield.

The investigation into the microwave irradiation power's effect led to the optimization of the reaction in glacial acetic acid, incorporating varied microwave power levels and durations as outlined in Table 2. The most favourable outcome was achieved using 200 W microwave power, resulting in the highest yield of 94 % within a short duration of 30 minutes (Table 2, entry 4). Therefore, the best-optimized condition was chosen for implementation in this protocol.

Table 3 Substrate scope of the synthesis of methoxy clubbed DHPQs **4a-v** [a, b]

5c, 50 %   6c, 28 %   5d, 18 %   6d, 46 %

5e, 44 %   6e, 35 %   5f, 22 %   6f, 53 %

5g, 48 %   6g, 30 %   5h, 41 %   6h, 32 %

5i, 47 %   6i, 28 %   5j, 61 %   6j, 18 %
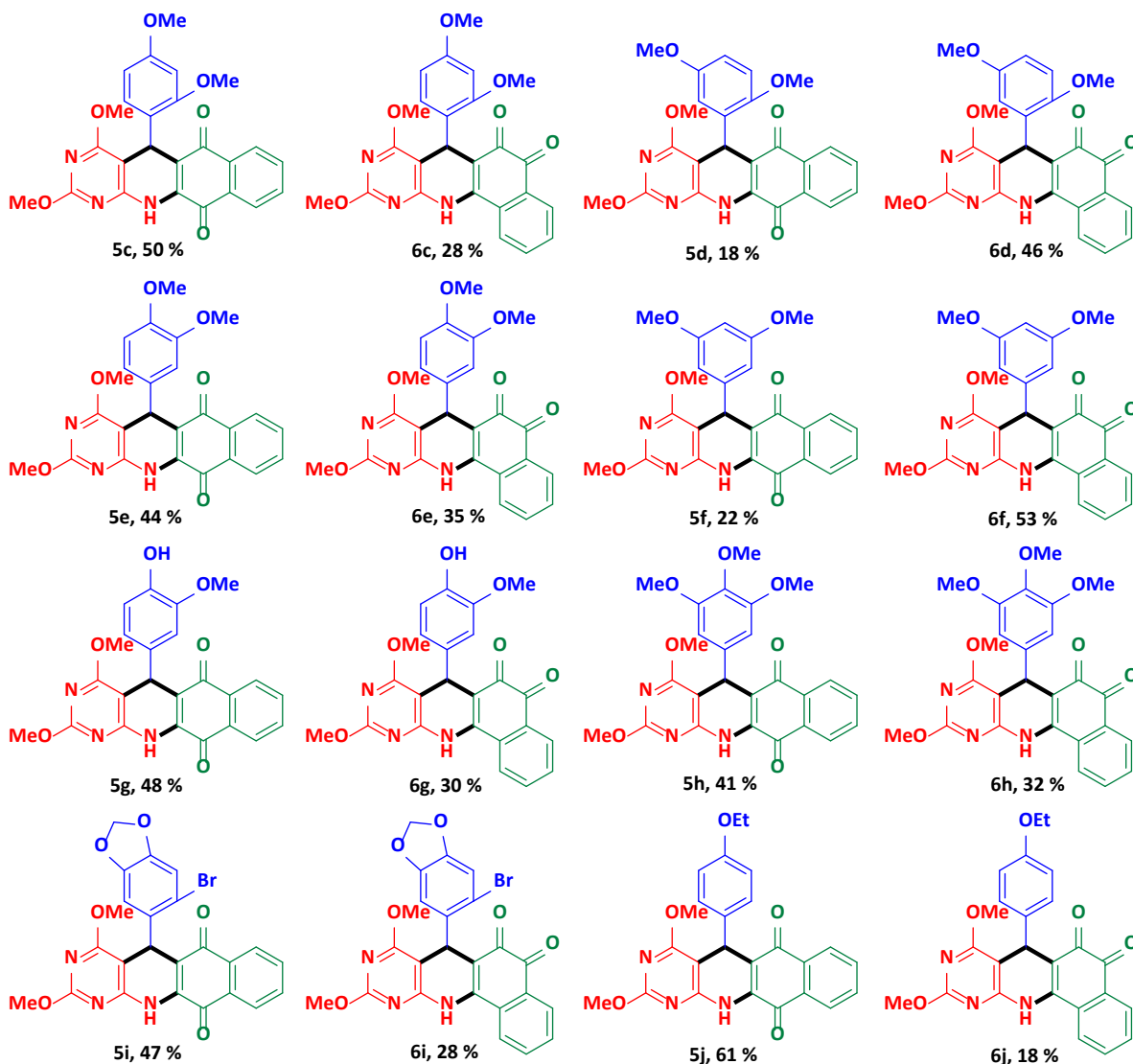
[a] Reaction condition: 2 mmol aldehyde **1**, 2 mmol 6-amino-2,4-dimethoxypyrimidine **2** and 2 mmol dimedone **3**, 5 mL acetic acid, 200 W MW, 30 min, Reflux

[b] Isolated yields are mentioned with the product

Having defined the reaction conditions, our focus shifted to an in-depth exploration of the substrate scope, covering **4a-j** and **5a-j** as shown in table 3. To achieve access to a wide array of structurally diverse methoxy clubbed DHPQs, the reaction was performed employing different substituted aryl aldehyde **1a-j**, 6-amino-2,4-dimethoxypyrimidine **2** and lawsone **3**. To assess their structural features, all synthesized compounds were characterised by ^{1}H nuclear magnetic resonance (NMR), ^{13}C NMR and liquid chromatography-mass spectrometry (LCMS) analyses.

Scheme 2 involved an exploration of possible reaction mechanisms to elucidate the formation of the product. Initially, the Knoevenagel condensation took place between an aromatic aldehyde and lawsone in the presence of acetic acid under microwave irradiation. This

process resulted in the formation of a potential Knoevenagel adduct (K) through the elimination of the first water molecule. Following this, 6-amino-2,4-dimethoxy aniline actively participated in a nucleophilic attack (C-H activation) on the Knoevenagel adduct (K), generating an imine derivative. In the concluding step, the imine derivative underwent an intramolecular ring-closing reaction through C–N bond formation, leading to the furnished linear and angular isomer product with the elimination of a second water molecule in the presence of acetic acid.
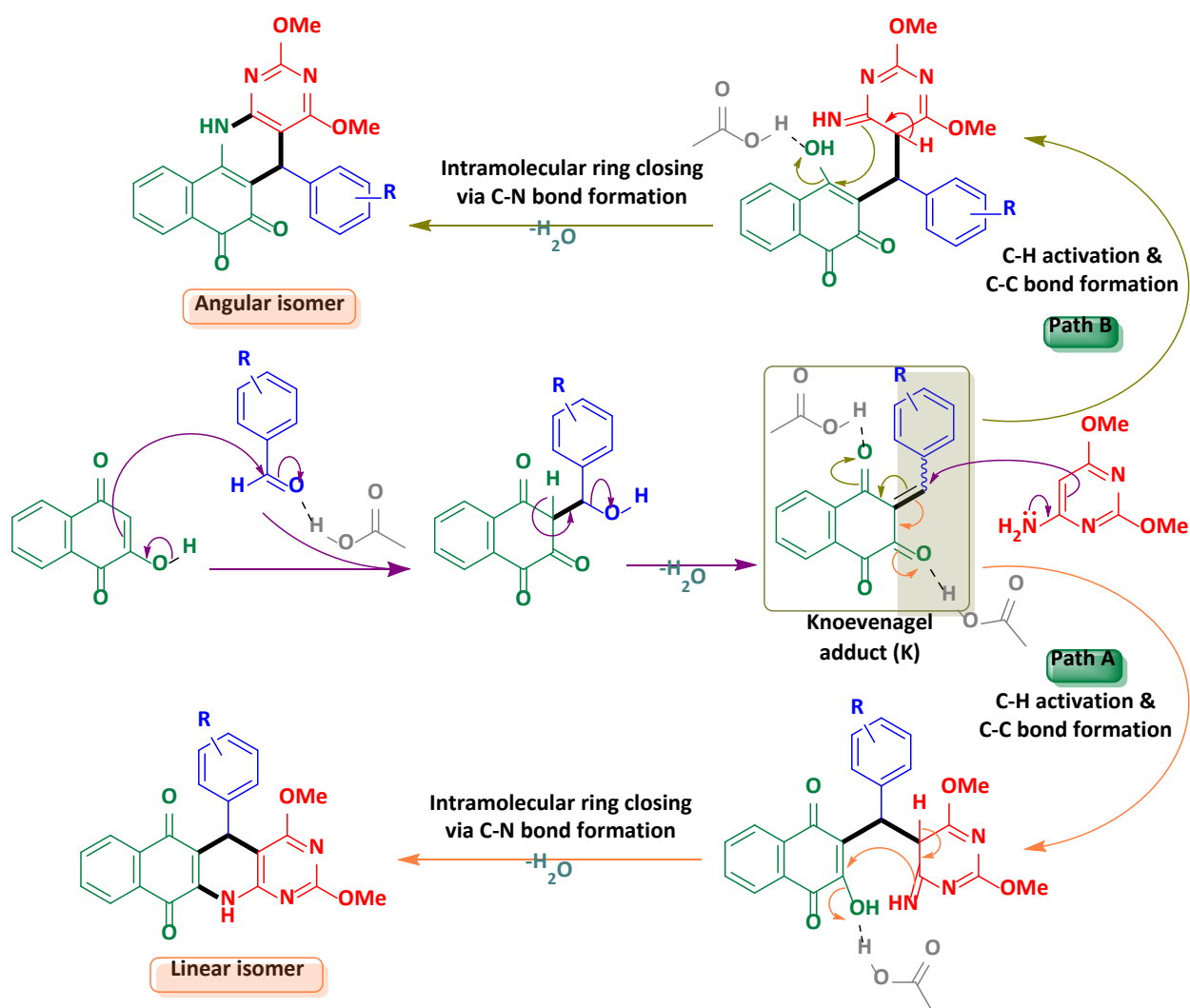

Scheme 2. Plausible reaction pathways.

2.2. Biological activity

2.2.1 Establishing a potential relationship between structure and biological anti-cancer activity of new molecules.

Primary patient derived glioblastoma cells GBM6, GBM22 and GBM143, were used to assess the anti-cancer properties of the panel of 20 compounds in vitro using cell viability assays.

All the compounds were tested at 10 µM, and the results showed that most of the series 5 compounds exhibited potent anti-cancer activity, compared to compounds of series 6 (Figure 2A-C). Compounds **6a**, **5b**, **5c**, **5d**, and **5h** negatively affected cell viability at least in two of the three cell lines (Figure 2A-C). To further determine **6a**, **5b**, **5c**, **5d**, and **5h** anti-cancer activities for GBM cells, we established the EC-50 for the molecules in GBM6 cell line. The EC-50 was determined by treating GBM6 cells at various concentrations of the drugs, starting from 50 nM up to 10 µM concentrations. After 48 h incubation, cell viability was measured and compounds **5c** and **5h** exhibited the most potent EC50 values at 2.9 µM and 3.3 µM respectively. (Figure 2D).
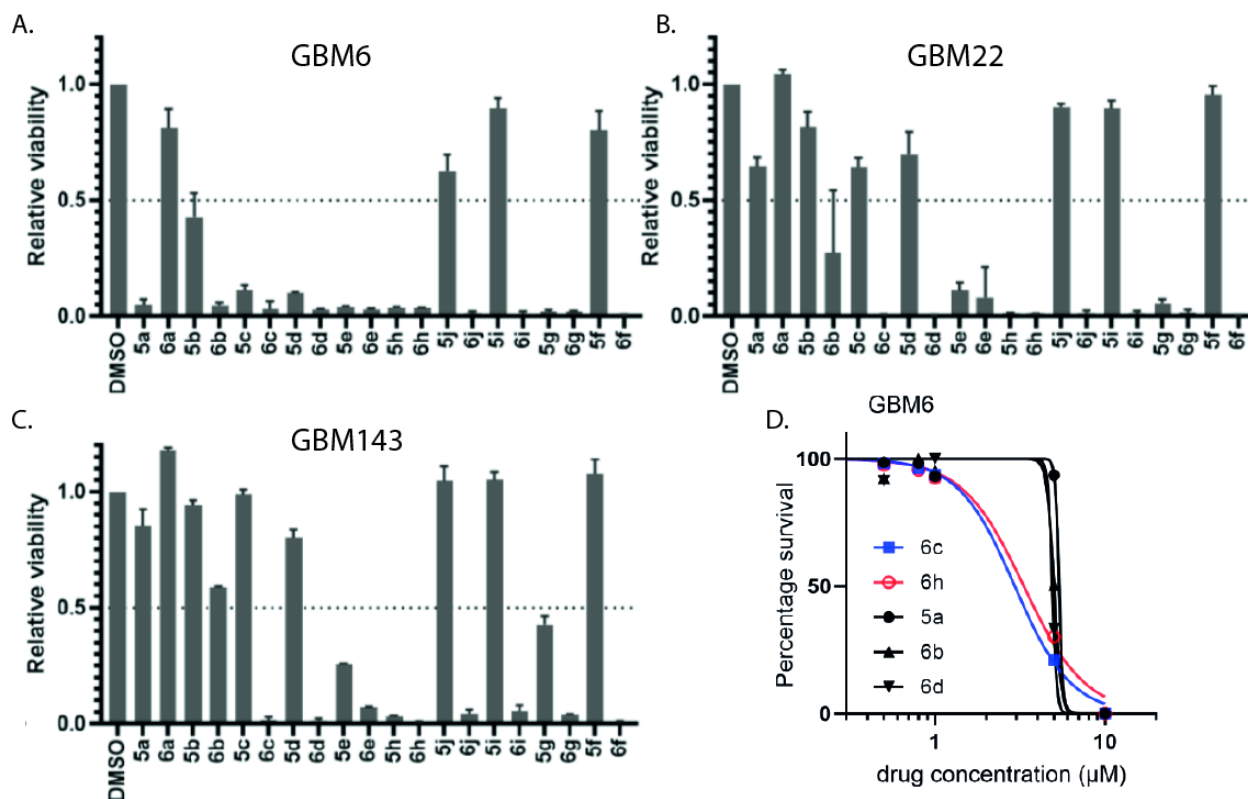
Figure 2. 6c and **6h** exhibits anti-cancer activity in diverse primary glioblastoma cell cultures. (A) GBM6, (B) GBM22, and (C) GBM143 cells were treated with a 10 µM doses of **5a-6f** for 72 hours and their viability was measured using CellTiter 96 AQueous Non-Radioactive Cell Proliferation Assay kit. Viability of DMSO-treated cells was used as control. Data are represented as fold viability of DMSO-treated control for each cell line with n=3 biological replicates. (D) GBM6 cells were treated with various doses of **6a**, **5b**, **5c**, **5d**, and **5h** and viability of cells were measured as in (C).

2.2.2 Anti-proliferative and anti-invasive effects of 5c and 5h in primary high grade glioma cell line

To establish the long-term effect of **5c** and **5h** on GBM cell proliferation, we carried out a cell proliferation assay at EC50 values of the respective molecules. A significant decrease in GBM6

proliferation was observed till 96 hours of treatment with both **5c** and **5h** compared to DMSO control (Figure 3A). Collectively, these results indicate that both **5c** and **5h** are promising anti-cancer drugs with ability to inhibit cancer cell proliferation at low concentrations. Thereafter, effect on cell invasion was tested using 3D spheroid invasion assay. **5h** failed to inhibit spheroid invasion at 3.3 µM concentration. **5c** exhibited moderate effect on spheroid invasion after day 4 which was statistically significant (p= 0.0112) (Figure 3B&C). Hence higher concentration of **5c** was tested again at 5 µM for the same spheroid invasion assay. At this concentration there was complete inhibition of 3D invasion with reduction in spheroid size indicating that **5c** not only inhibited cell invasion but also spheroid growth (Figure 3D). Interestingly, **5c** treatment leads to ablation of phospho STAT3 signal at low concentrations and phospho ERK and phospho AKT signals at higher concentrations (Figure 3E). **5c** treatment for 16hr also leads to significant increase in S and G2-phase cells in the cell cycle (Figure 3F). Furthermore, colony-formation assay shows that **5c** at 3 µM is more potent than glioma clinical drug temozolomide at 50 µM (Figure 3G).
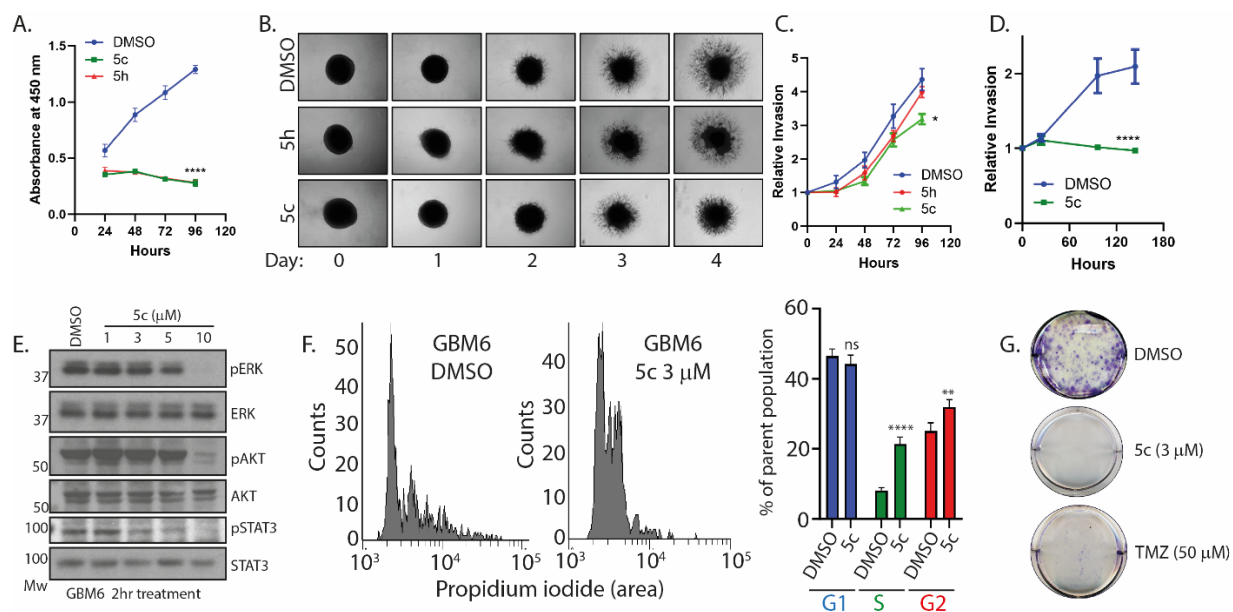
Figure 3. Effect of **5c** and **5h** compounds on proliferation and invasion in GBM cells: (A) GBM6 cell proliferation was measured over 5 days in the presence or absence of **5c** or **5h**. Error bar indicates standard error calculated from three independent experiments in triplicate; ****p<0.0001. (B) Panel of representative images of spheroids generated from GBM6 cells, invading basement membrane matrix post treatment with DMSO in control group and **5c** at 2.9 µM concentration and **5h** at 3.3 µM concentration in test groups, respectively. Photomicrographs of each spheroid was taken at x100 at different time points. Relative invasion was calculated and quantified (C). (D) Quantification and (E) representative images of invasion in DMSO treated control and **5c** at 5 µM concentration at day 0 and day 6. Statistically significant difference is represented as *p< 0.05, and ****p<0.0001. (F) Western blot analysis was carried out with the indicated antibodies for GBM6 cell lysates treated with **5c** for the indicated concentrations for 2

hr. (G) Asynchronous GBM6 cells were treated with various doses of **5c** for 16 hours and the cell cycle distribution was analysed using propidium iodide and quantified using flow cytometry. Statistically significant difference is represented as **p< 0.01, and ****p<0.0001 compared to DMSO-treated control cell population; two-way ANOVA with Sidak's multiple comparison; ns: not significant. (H) GBM143 colony formation assay with or without treatment with **5c** or temozolomide (TMZ) over 15 days.

3. Experimental section

3.1. General methods:

For synthesis, all chemical reagents were purchased from the TCI, Sigma - Aldrich and Sisco Research Laboratories Pvt. Ltd. and used without further purification. The microwave-assisted reactions were performed in a "SINEO UWave-1000 Microwave, UV, US Synthesis Extraction Reactor". The progress of all chemical reactions was monitored by thin-layer chromatography (TLC, on aluminium plates pre-coated with F254 silica gel 60). Melting points of all solid compounds were determined by the open capillary tube method and are uncorrected. The LCMS analysis was collected on an MS–Agilent 6120 quadrupole. Nuclear magnetic resonance spectra (^{1}H NMR & ^{13}C NMR) were recorded on a Bruker 400 MHz WB FT-NMR spectrometer having proton noise decoupling mode with a standard 5mm probe using CDCl$_3$ and DMSO-d6 solution. Abbreviations are used for the ^{1}H NMR signal are as follows: s = singlet, d = doublet, t = triplet, q = quartet, dd = doublet of doublets, td = triplet of doublets, qd = quartet of doublets, qt = quartet of triplet,s m = multiplet. The chemical shifts are reported in parts per million and coupling constants (*J*) are provided in Hertz.

3.2. General procedure for synthesis of alkoxy-functionalised DHPQs 5a-j and 6a-j.

A mixture of aromatic aldehydes (**1**, 1 mmol), 6-amino-2,4-dimethoxypyrimidine (**2**, 1 mmol), lawsone (**3**, 1 mmol) and acetic acid (5 mL) were charged into a microwave vessel. The reaction mixture was heated at 110 °C (200 W) by MW irradiation for 30 min. The reaction progress was monitored on TLC using n-hexane:ethyl acetate (50:50, v/v) as mobile phase. After complete consumption of starting material, the reaction mixture was cooled to room temperature and poured into 20 mL cold water for complete solidification. The obtained crude product was filtered and dried in an oven. Further isolation and purification, the crude product was separated by flash chromatography using 50% ethyl acetate and 50% n-hexane as a mobile phase.

3.2.1. 2,4-dimethoxy-5-(4-methoxyphenyl)-5,12-dihydrobenzo[*g*]pyrimido[4,5-*b*]quinoline-6,11-dione (5a)

Brownish orange solid, mp. 220 – 222 °C; ^{1}H-NMR (400 MHz, DMSO-d$_6$) (δ, ppm): 10.78 (s, 1H, NH), 8.52 (d, *J* = 8.0 Hz, 1H, ArH), 7.98 (d, *J* = 7.3 Hz, 1H, ArH), 7.83 (t, *J* = 7.5 Hz, 1H, ArH), 7.67 (t, *J* = 7.6 Hz, 1H, ArH), 7.14 (d, *J* = 8.6 Hz, 2H, ArH), 6.77 (d, *J* = 8.6 Hz, 2H, ArH), 5.16 (s,

1H,CH), 3.93 (s, 3H, OCH$_3$), 3.89 (s, 3H, OCH$_3$), 3.65 (s, 3H, OCH$_3$); ^{13}C-NMR (100 MHz, DMSO-d$_6$) (δ, ppm): 179.18, 176.41, 168.67, 163.79, 159.52, 156.65, 146.81, 146.40, 135.27, 131.69, 131.08, 130.15, 129.88, 129.13, 125.25, 120.03, 114.30, 113.78, 111.79, 95.70, 55.34, 55.07, 54.71, 34.24; LCMS(ES+): 430.48 [M + H]$^+$.

3.2.2. 8,10-dimethoxy-7-(4-methoxyphenyl)-7,12-dihydrobenzo[*h*]pyrimido[4,5-*b*]quinoline-5,6-dione (6a)

Orange solid, mp. 228 – 230 °C; ^{1}H-NMR (400 MHz, DMSO-d$_6$) (δ, ppm): 9.91 (s, 1H, NH), 8.03 (dd, *J* = 6.8, 2.0 Hz, 1H, ArH), 7.91 (dd, *J* = 6.9, 1.9 Hz, 1H, ArH), 7.81 (pd, *J* = 7.3, 1.7 Hz, 2H, ArH), 7.20 – 7.12 (m, 2H, ArH), 6.81 – 6.74 (m, 2H, ArH), 5.27 (s, 1H, CH), 3.89 (s, 3H, OCH$_3$), 3.86 (s, 3H, OCH$_3$), 3.65 (s, 3H, OCH$_3$); ^{13}C-NMR (100 MHz, DMSO-d$_6$) (δ, ppm): 181.51, 179.06, 168.12, 163.24, 157.92, 155.83, 139.25, 137.16, 134.75, 133.32, 131.76, 130.34, 128.65, 125.93, 125.63, 118.26, 113.71, 94.32, 54.94, 54.42, 54.10, 33.64; LCMS(ES+): 430.47 [M + H]$^+$.

3.2.3. 2,4-dimethoxy-5-(3-methoxyphenyl)-5,12-dihydrobenzo[*g*]pyrimido[4,5-*b*]quinoline-6,11-dione (5b)

Brownish orange solid, mp. 222 – 224 °C; ^{1}H-NMR (400 MHz, DMSO-d$_6$) (δ, ppm): δ 9.97 (s, 1H. NH), 8.07 – 8.01 (m, 1H, ArH), 7.92 (dd, *J* = 7.2, 1.9 Hz, 1H, ArH), 7.83 (qd, *J* = 7.0, 1.8 Hz, 2H, ArH), 7.18 – 7.11 (m, 1H, ArH), 6.85 – 6.69 (m, 2H, ArH), 5.31 (s, 1H, CH), 3.89 (s, 2H, OCH$_3$), 3.88 (s, 3H, OCH$_3$), 3.68 (s, 3H, OCH$_3$); ^{13}C-NMR (100 MHz, DMSO-d$_6$) (δ, ppm): 178.70, 175.93, 168.19, 163.31, 159.04, 156.17, 146.33, 145.92, 134.79, 131.21, 130.60, 129.67, 129.39, 128.65, 124.77, 119.55, 113.82, 113.29, 111.30, 95.22, 54.86, 54.59, 54.23, 33.75; LCMS(ES+): 430.20 [M + H]$^+$.

3.2.4. 8,10-dimethoxy-7-(3-methoxyphenyl)-7,12-dihydrobenzo[*h*]pyrimido[4,5-*b*]quinoline-5,6-dione (6b)

Orange solid, mp. 230 – 232 °C; ^{1}H-NMR (400 MHz, DMSO-d$_6$) (δ, ppm): 9.99 (s, 1H, NH), 8.06 – 8.02 (m, 1H, ArH), 7.94 – 7.90 (m, 1H, ArH), 7.86 – 7.78 (m, 2H, ArH), 7.14 (t, *J* = 8.2 Hz, 1H, ArH), 6.83 – 6.79 (m, 2H, ArH), 6.74 – 6.70 (m, 1H, ArH), 5.31 (s, 1H,CH), 3.89 (s, 3H, OCH$_3$), 3.88 (s, 3H, OCH$_3$), 3.68 (s, 3H, OCH$_3$); ^{13}C-NMR (100 MHz, DMSO-d$_6$) (δ, ppm): 181.95, 179.47, 168.65, 163.81, 159.60, 156.44, 146.70, 140.10, 135.24, 133.82, 132.24, 130.88, 129.96, 126.45, 126.16, 120.30, 118.30, 114.39, 112.00, 94.47, 55.39, 54.94, 54.61, 34.98; LCMS(ES+): 430.24 [M + H]$^+$.

3.2.5. 5-(2,4-dimethoxyphenyl)-2,4-dimethoxy-5,12-dihydrobenzo[*g*]pyrimido[4,5-*b*]quinoline-6,11-dione (5c)

Brownish orange solid, mp. 218 – 220 °C; ^{1}H-NMR (400 MHz, DMSO-d$_6$) (δ, ppm): δ 10.72 (s, 1H, NH), 8.52 (d, *J* = 8.1 Hz, 1H, ArH), 7.95 (d, *J* = 7.5 Hz, 2H, ArH), 7.65 (t, *J* = 7.5 Hz, 1H, ArH), 7.19 (d, *J* = 8.1 Hz, 1H, ArH), 6.41 (d, *J* = 7.8 Hz, 2H, ArH), 5.21 (s, 1H, NH), 3.91 (s, 3H, OCH$_3$), 3.82 (s, 3H, OCH$_3$), 3.67 (s, 3H, OCH$_3$), 3.60 (s, 3H, OCH$_3$); ^{13}C-NMR (100 MHz, DMSO-d$_6$) (δ, ppm): 179.01, 175.75, 168.01, 162.90, 159.23, 158.51, 156.53, 146.13, 134.85, 131.38, 130.99, 130.50,

130.06, 128.52, 124.72, 124.56, 112.71, 104.48, 98.91, 94.80, 55.51, 55.04, 54.45, 54.03, 31.61; LCMS(ES+): 460.25 [M + H]$^+$.

3.2.6. 7-(2,4-dimethoxyphenyl)-8,10-dimethoxy-7,12-dihydrobenzo[*h*]pyrimido[4,5-*b*]quinoline-5,6-dione (6c)

Orange solid, mp. 232 – 234 °C; ^{1}H-NMR (400 MHz, DMSO-d$_6$) (δ, ppm): 9.76 (s, 1H, NH), 8.05 – 7.98 (m, 1H, ArH), 7.81 (dqd, *J* = 21.9, 7.5, 1.7 Hz, 4H, ArH), 7.21 – 7.14 (m, 1H, ArH), 6.44 – 6.37 (m, 2H, ArH), 5.39 (s, 1H, CH), 3.86 (s, 3H, OCH$_3$), 3.79 (s, 3H, OCH$_3$), 3.68 (s, 3H, OCH$_3$), 3.65 (s, 3H, OCH$_3$); ^{13}C-NMR (100 MHz, DMSO-d$_6$) (δ, ppm): 181.84, 179.75, 168.43, 163.41, 159.85, 158.87, 156.70, 140.15, 135.24, 133.60, 132.35, 131.57, 130.58, 126.29, 126.04, 125.63, 117.91, 105.22, 99.26, 94.21, 56.01, 55.51, 54.76, 54.37, 32.03; LCMS(ES+): 460.25 [M + H]$^+$.

3.2.7. 5-(2,5-dimethoxyphenyl)-2,4-dimethoxy-5,12-dihydrobenzo[*g*]pyrimido[4,5-*b*]quinoline-6,11-dione (5d)

Brownish orange solid, mp. 218 – 220 °C; ^{1}H-NMR (400 MHz, DMSO-d$_6$) (δ, ppm): δ 10.77 (s, 1H, NH), 8.53 (d, *J* = 8.0 Hz, 1H, ArH), 7.96 (dd, *J* = 7.6, 1.5 Hz, 1H, ArH), 7.83 (td, *J* = 7.7, 1.5 Hz, 1H, ArH), 7.69 – 7.63 (m, 1H, ArH), 6.86 (d, *J* = 3.1 Hz, 1H, ArH), 6.78 (d, *J* = 8.9 Hz, 1H, ArH), 6.69 (dd, *J* = 8.8, 3.1 Hz, 1H, ArH), 5.21 (s, 1H, CH), 3.91 (s, 3H, OCH$_3$), 3.83 (s, 3H, OCH$_3$), 3.67 (s, 3H, OCH$_3$), 3.54 (s, 3H, OCH$_3$); ^{13}C-NMR (100 MHz, DMSO-d$_6$) (δ, ppm): 178.94, 175.69, 168.05, 163.01, 156.57, 152.58, 152.06, 146.34, 134.82, 133.22, 131.05, 130.52, 129.95, 128.51, 124.58, 117.39, 113.12, 112.30, 111.75, 94.44, 56.21, 55.26, 54.45, 54.04, 32.63; LCMS(ES+): 460.29 [M + H]$^+$.

3.2.8. 7-(2,5-dimethoxyphenyl)-8,10-dimethoxy-7,12-dihydrobenzo[*h*]pyrimido[4,5-*b*]quinoline-5,6-dione (6d)

Orange solid, mp. 238 – 240 °C; ^{1}H-NMR (400 MHz, DMSO-d$_6$) (δ, ppm): 9.85 (s, 1H, NH), 8.05 – 7.98 (m, 1H, ArH), 7.89 – 7.75 (m, 3H, ArH), 6.86 – 6.79 (m, 2H, ArH), 6.70 (dd, *J* = 8.9, 3.0 Hz, 1H, ArH), 5.40 (s, 1H, CH), 3.86 (s, 3H, OCH$_3$), 3.80 (s, 3H, OCH$_3$), 3.67 (s, 3H, OCH$_3$), 3.59 (s, 3H, OCH$_3$); ^{13}C-NMR (100 MHz, DMSO-d$_6$) (δ, ppm): 181.75, 179.68, 168.47, 163.53, 156.76, 153.19, 152.43, 140.38, 135.25, 134.01, 133.61, 132.31, 130.59, 126.32, 126.07, 117.52, 113.53, 112.48, 93.88, 56.67, 55.72, 54.78, 54.39, 33.13; LCMS(ES+): 460.29 [M + H]$^+$.

3.2.9. 5-(3,4-dimethoxyphenyl)-2,4-dimethoxy-5,12-dihydrobenzo[*g*]pyrimido[4,5-*b*]quinoline-6,11-dione (5e)

Brownish orange solid, mp. 224 – 226 °C; ^{1}H-NMR (400 MHz, DMSO-d$_6$) (δ, ppm): δ 10.78 (s, 1H, NH), 8.51 (d, *J* = 8.0 Hz, 1H, ArH), 7.99 (d, *J* = 7.6 Hz, 1H, ArH), 7.83 (t, *J* = 7.6 Hz, 1H, ArH), 7.67 (t, *J* = 7.6 Hz, 1H, ArH), 6.90 (s, 1H, ArH), 6.77 (d, *J* = 8.5 Hz, 1H, ArH), 6.62 (d, *J* = 6.3 Hz, 1H, ArH), 5.17 (s, 1H, CH), 3.93 (s, 3H, OCH$_3$), 3.91 (s, 3H, OCH$_3$), 3.69 (s, 3H, OCH$_3$), 3.64 (s, 3H, OCH$_3$); ^{13}C-NMR (100 MHz, DMSO-d$_6$) (δ, ppm): 178.74, 176.01, 168.16, 163.19, 156.00, 148.25, 147.50,

145.66, 137.57, 134.76, 131.12, 130.57, 129.74, 128.61, 124.70, 119.03, 113.56, 111.85, 111.77, 95.54, 55.43, 54.54, 54.15, 33.23; LCMS(ES+): 460.24 [M + H]$^+$.

3.2.10. 7-(3,4-dimethoxyphenyl)-8,10-dimethoxy-7,12-dihydrobenzo[*h*]pyrimido[4,5-*b*]quinoline-5,6-dione (6e)

Orange solid, mp. 238 – 240 °C; ^{1}H-NMR (400 MHz, DMSO-d$_6$) (δ, ppm): 9.94 (s, 1H, NH), 8.04 (d, *J* = 6.5 Hz, 1H, ArH), 7.92 (d, *J* = 7.0 Hz, 1H, ArH), 7.85-7.78 (m, 2H, ArH), 6.89 (s, 1H, ArH), 6.77 (d, *J* = 8.4 Hz, 1H, ArH), 6.68 (d, *J* = 8.2 Hz, 1H, ArH), 5.26 (s, 1H, CH), 3.89 (s, 6H, OCH$_3$), 3.70 (s, 3H, OCH$_3$), 3.64 (s, 3H, OCH$_3$); ^{13}C-NMR (100 MHz, DMSO-d$_6$) (δ, ppm): 179.06, 168.14, 163.22, 155.78, 148.31, 147.60, 139.40, 137.51, 134.74, 133.32, 131.80, 130.41, 125.95, 125.66, 119.54, 118.02, 111.79, 111.66, 94.33, 55.45, 55.41, 54.44, 54.08, 34.02; LCMS(ES+): 460.24 [M + H]$^+$.

3.2.11. 5-(3,5-dimethoxyphenyl)-2,4-dimethoxy-5,12-dihydrobenzo[*g*]pyrimido[4,5-*b*]quinoline-6,11-dione (5f)

Brownish orange solid, mp. 222 – 224 °C; ^{1}H-NMR (400 MHz, DMSO-d$_6$) (δ, ppm): δ 10.78 (s, 1H, NH), 8.54 (d, *J* = 8.0 Hz, 1H, ArH), 7.97 (d, *J* = 7.6 Hz, 1H, ArH), 7.84 (t, *J* = 7.7 Hz, 1H, ArH), 6.87 (d, *J* = 3.1 Hz, 1H, ArH), 6.79 (d, *J* = 8.9 Hz, 1H, ArH), 6.70 (dd, *J* = 8.8, 3.1 Hz, 1H, ArH), 5.22 (s, 1H, CH), 3.92 (s, 3H, OCH$_3$), 3.84 (s, 3H, OCH$_3$), 3.68 (s, 3H, OCH$_3$), 3.55 (s, 3H, OCH$_3$); ^{13}C-NMR (100 MHz, DMSO-d$_6$) (δ, ppm): 179.42, 176.17, 168.53, 163.49, 157.05, 153.07, 152.54, 146.83, 135.30, 133.71, 131.53, 131.00, 130.43, 128.99, 125.06, 117.88, 113.60, 112.79, 112.23, 94.93, 56.70, 55.74, 54.93, 54.52, 33.11; LCMS(ES+): 460.48 [M + H]$^+$.

3.2.12. 7-(3,5-dimethoxyphenyl)-8,10-dimethoxy-7,12-dihydrobenzo[*h*]pyrimido[4,5-*b*]quinoline-5,6-dione (6f)

Orange solid, mp. 236 – 238 °C; ^{1}H-NMR (400 MHz, DMSO-d$_6$) (δ, ppm): 9.86 (s, 1H, NH), 8.03 (d, *J* = 6.6 Hz, 1H, ArH), 7.87 (d, *J* = 7.1 Hz, 1H, ArH), 7.84-7.78 (m, 2H, ArH), 6.85 (d, *J* = 3.1 Hz, 1H, ArH), 6.82 (d, *J* = 8.9 Hz, 1H, ArH), 6.71 (dd, *J* = 8.9, 3.0 Hz, 1H, ArH), 5.40 (s, 1H, CH), 3.87 (s, 3H, OCH$_3$), 3.81 (s, 3H, OCH$_3$), 3.67 (s, 3H, OCH$_3$), 3.60 (s, 3H, OCH$_3$); ^{13}C-NMR (100 MHz, DMSO-d$_6$) (δ, ppm): 181.33, 179.24, 167.92, 162.90, 159.34, 158.36, 156.20, 139.64, 134.73, 133.09, 131.84, 131.06, 130.08, 125.78, 125.53, 125.12, 117.40, 104.71, 98.76, 93.70, 55.50, 55.01, 54.25, 53.86, 31.52; LCMS(ES+): 460.48 [M + H]$^+$.

3.2.13. 5-(4-hydroxy-3-methoxyphenyl)-2,4-dimethoxy-5,12-dihydrobenzo[*g*]pyrimido[4,5-*b*]quinoline-6,11-dione (5g)

Brownish orange solid, mp. 252 – 254 °C; ^{1}H-NMR (400 MHz, DMSO-d$_6$) (δ, ppm): δ 10.74 (s, 1H, NH), 8.77 (s, 1H, OH), 8.51 (d, *J* = 8.0 Hz, 1H, ArH), 7.99 (d, *J* = 7.7 Hz, 1H, ArH), 7.83 (t, *J* = 7.5 Hz, 1H, ArH), 7.67 (t, *J* = 7.5 Hz, 1H, ArH), 6.87 (s, 1H, ArH), 6.59 (d, *J* = 8.1 Hz, 1H, ArH), 6.51 (d, *J* = 8.1 Hz, 1H, ArH), 5.14 (s, 1H, CH), 3.93 (s, 3H, OCH$_3$), 3.92 (s, 3H, OCH$_3$), 3.70 (s, 3H, OCH$_3$); ^{13}C-NMR (100 MHz, DMSO-d$_6$) (δ, ppm): 178.80, 176.00, 168.15, 163.13, 156.00, 147.04, 145.65,

145.24, 136.05, 134.77, 131.08, 130.56, 129.83, 128.61, 124.69, 119.28, 115.30, 113.72, 112.10, 95.77, 55.55, 54.54, 54.13, 33.12; LCMS(ES+): 446.44 [M + H]$^+$.

3.2.14.   7-(4-hydroxy-3-methoxyphenyl)-8,10-dimethoxy-7,12-dihydrobenzo[*h*]pyrimido[4,5-*b*]quinoline-5,6-dione (6g)

Orange solid, mp. 234 – 236 °C; ^{1}H-NMR (400 MHz, DMSO-d$_6$) (δ, ppm): 9.86 (s, 1H, NH), 8.81 (s, 1H, OH), 8.04 (dd, *J* = 7.3, 1.6 Hz, 1H, ArH), 7.92 (dd, *J* = 7.4, 1.6 Hz, 1H, ArH), 7.81 (pd, *J* = 7.4, 1.6 Hz, 2H, ArH), 6.85 (d, *J* = 1.9 Hz, 1H, ArH), 6.62 – 6.54 (m, 2H, ArH), 5.23 (s, 1H, CH), 3.89 (s, 3H, OCH$_3$), 3.88 (s, 3H, OCH$_3$), 3.71 (s, 3H, OCH$_3$); ^{13}C-NMR (100 MHz, DMSO-d$_6$) (δ, ppm): 181.58, 179.06, 168.12, 163.15, 155.72, 147.14, 145.40, 139.26, 135.99, 134.72, 133.27, 131.81, 130.38, 125.91, 125.65, 119.80, 118.20, 115.33, 112.04, 94.48, 55.59, 54.39, 54.02, 33.86; LCMS(ES+): 446.44 [M + H]$^+$.

3.2.15.   2,4-dimethoxy-5-(3,4,5-trimethoxyphenyl)-5,12-dihydrobenzo[*g*]pyrimido[4,5-*b*]quinoline-6,11-dione (5h)

Brownish orange solid, mp. 220 – 222 °C; ^{1}H-NMR (400 MHz, DMSO-d$_6$) (δ, ppm): δ 10.76 (s, 1H, NH), 8.51 (d, *J* = 7.9 Hz, 1H, ArH), 8.00 (dd, *J* = 7.6, 1.5 Hz, 1H, ArH), 7.83 (td, *J* = 7.7, 1.5 Hz, 1H, ArH), 7.67 (td, *J* = 7.5, 0.9 Hz, 1H, ArH), 6.50 (s, 2H, ArH), 5.19 (s, 1H, CH), 3.94 (s, 3H, OCH$_3$), 3.93 (s, 3H, OCH$_3$), 3.66 (s, 6H, OCH$_3$), 3.57 (s, 3H, OCH$_3$); ^{13}C-NMR (100 MHz, DMSO-d$_6$) (δ, ppm): 179.10, 176.42, 168.65, 163.71, 156.43, 153.05, 146.32, 140.93, 136.78, 135.16, 131.56, 131.10, 130.11, 129.03, 125.19, 113.57, 105.31, 105.03, 95.73, 60.31, 56.23, 55.01, 54.60, 34.52; LCMS(ES+): 490.28 [M + H]$^+$.

3.2.16.   8,10-dimethoxy-7-(3,4,5-trimethoxyphenyl)-7,12-dihydrobenzo[*h*]pyrimido[4,5-*b*]quinoline-5,6-dione (6h)

Orange solid, mp. 228 – 230 °C; ^{1}H-NMR (400 MHz, DMSO-d$_6$) (δ, ppm): 9.92 (s, 1H, NH), 8.06 (dd, *J* = 6.9, 2.0 Hz, 1H, ArH), 7.94 (dd, *J* = 6.9, 1.9 Hz, 1H, ArH), 7.84 (qt, *J* = 7.4, 3.6 Hz, 2H, ArH), 6.54 (s, 2H, ArH), 5.29 (s, 1H, CH), 3.92 (s, 3H, OCH$_3$), 3.90 (s, 3H, OCH$_3$), 3.69 (s, 6H, OCH$_3$), 3.58 (s, 3H, OCH$_3$); ^{13}C-NMR (100 MHz, DMSO-d$_6$) (δ, ppm): 181.25, 179.17, 167.96, 163.03, 156.25, 152.69, 151.92, 139.88, 134.75, 133.50, 133.11, 131.80, 130.08, 125.81, 125.56, 117.01, 113.02, 111.98, 93.38, 56.17, 55.22, 54.27, 53.89, 32.63; LCMS(ES+): 490.28 [M + H]$^+$.

3.2.17.   5-(6-bromobenzo[*d*][1,3]dioxol-5-yl)-2,4-dimethoxy-5,12-dihydrobenzo[*g*]pyrimido[4,5-*b*]quinoline-6,11-dione (5i)

Brownish orange solid, mp. 252 – 254 °C; ^{1}H-NMR (400 MHz, DMSO-d$_6$) (δ, ppm): δ 10.72 (s, 1H, NH), 7.99 (dd, *J* = 7.6, 1.5 Hz, 1H, ArH), 7.89 – 7.82 (m, 2H, ArH), 7.68 (dd, *J* = 8.3, 6.0 Hz, 2H, ArH), 7.04 (s, 1H, ArH), 6.77 (s, 1H, ArH), 5.95 (s, 2H, OCH$_2$O), 5.45 (s, 1H, CH), 3.92 (s, 3H, OCH$_3$), 3.83 (s, 3H, OCH$_3$); ^{13}C-NMR (100 MHz, DMSO-d$_6$) (δ, ppm): 179.11, 176.36, 168.96,

163.82, 156.30, 147.64, 147.22, 146.33, 137.85, 135.21, 131.68, 131.14, 130.18, 128.98, 126.19, 125.53, 113.84, 112.24, 110.63, 102.29, 95.41, 55.04, 54.38, 35.78; LCMS(ES+): 522.16 [M + H]$^+$.

3.2.18. 7-(6-bromobenzo[d][1,3]dioxol-5-yl)-8,10-dimethoxy-7,12-dihydrobenzo[h]pyrimido[4,5-b]quinoline-5,6-dione (6i)

Orange solid, mp. 224 – 226 °C; ^{1}H-NMR (400 MHz, DMSO-d$_6$) (δ, ppm): 9.91 (s, 1H, NH), 8.03 (s, 1H, ArH), 7.89 (s, 1H, ArH), 7.82 (d, J = 6.0 Hz, 2H, ArH), 7.07 (s, 1H, ArH), 6.80 (s, 1H, ArH), 5.95 (s, 2H, OCH$_2$O), 5.60 (s, 1H, CH), 3.88 (s, 3H, OCH$_3$), 3.81 (s, 3H, OCH$_3$); ^{13}C-NMR (100 MHz, DMSO-d$_6$) (δ, ppm): 181.22, 178.94, 168.41, 163.33, 155.51, 147.31, 146.82, 139.84, 137.70, 134.71, 133.18, 131.76, 130.28, 125.85, 125.62, 117.67, 113.00, 111.73, 110.19, 101.83, 93.92, 54.41, 53.77, 35.60; LCMS(ES+): 522.18 [M + H]$^+$.

3.2.19. 5-(4-ethoxyphenyl)-2,4-dimethoxy-5,12-dihydrobenzo[g]pyrimido[4,5-b]quinoline-6,11-dione (5j)

Brownish orange solid, mp. 226 – 228 °C; ^{1}H-NMR (400 MHz, DMSO-d$_6$) (δ, ppm): δ 10.80 (s, 1H, NH), 8.52 (d, J = 7.9 Hz, 1H, ArH), 7.98 (d, J = 7.6 Hz, 1H, ArH), 7.83 (t, J = 7.7 Hz, 1H, ArH), 7.67 (t, J = 7.6 Hz, 1H, ArH), 7.12 (d, J = 8.3 Hz, 2H, ArH), 6.75 (d, J = 8.3 Hz, 2H, ArH), 5.15 (s, 1H, CH), 3.93 (s, 3H, OCH$_3$), 3.91 (d, J = 6.9 Hz, 2H, CH$_2$), 3.89 (s, 3H, OCH$_3$), 1.25 (t, J = 7.0 Hz, 3H, CH$_3$); ^{13}C-NMR (100 MHz, DMSO-d$_6$) (δ, ppm): 178.76, 175.93, 168.16, 163.21, 157.09, 156.04, 145.60, 137.06, 134.78, 131.13, 130.54, 129.76, 128.62, 128.42, 124.73, 114.07, 113.81, 95.64, 62.83, 54.55, 54.18, 32.94, 14.62; LCMS(ES+): 444.24 [M + H]$^+$.

3.2.20. 7-(4-ethoxyphenyl)-8,10-dimethoxy-7,12-dihydrobenzo[h]pyrimido[4,5-b]quinoline-5,6-dione (6j)

Orange solid, mp. 208 – 210 °C; ^{1}H-NMR (400 MHz, DMSO-d$_6$) (δ, ppm): 9.95 (s, 1H, NH), 8.05 – 8.01 (m, 1H, ArH), 7.93 – 7.89 (m, 1H, ArH), 7.81 (pd, J = 7.3, 1.7 Hz, 2H, ArH), 7.14 (d, J = 8.7 Hz, 2H, ArH), 6.76 (d, J = 8.7 Hz, 2H, ArH), 5.26 (s, 1H, CH), 3.92 (m, 2H, CH$_2$), 3.89 (s, 3H, OCH$_3$), 3.86 (s, 3H, OCH$_3$), 1.25 (t, J = 7.0 Hz, 3H, CH$_3$); ^{13}C-NMR (100 MHz, DMSO-d$_6$) (δ, ppm): 181.50, 179.05, 168.11, 163.22, 157.21, 155.84, 139.24, 136.99, 134.74, 133.31, 131.76, 130.34, 128.61, 125.92, 125.62, 118.27, 114.15, 94.32, 62.83, 54.40, 54.07, 33.59, 14.61; LCMS(ES+): 444.27 [M + H]$^+$.

3.3. Cell Based Assays

3.3.1 Materials and cell lines

Primary patient glioblastoma cells GBM6, GBM22 and GBM143 were acquired from the Brain Tumour PDX National Resource, Mayo Clinic, USA. Propidium iodide, insulin and epidermal growth factor were purchased from Sigma Millipore. Temozolomide was from Accord Healthcare. Immunoblot analyses were carried out as stated previously[44-46]. The following antibodies were used for immunoblotting: total AKT (Cell Signalling #9272), phospho Thr308 AKT (Cell Signalling #2965), total p44/42 ERK1/2 (Cell Signalling #4695), phospho Thr202/Tyr204 p44/42 ERK1/2 (Cell

3.3.2 Cell Culture

Mammalian cells were grown in a humidified incubator with 5% CO_2 at 37°C. Primary patient glioblastoma cell lines were cultured in GBM media (DMEM supplemented with 10% FBS, 1% penicillin and streptomycin, 10 µg/ml insulin, and 20 ng/ml hEGF) as reported previously[6, 7, 47].

3.3.3 Cell viability assay

Cell viability was measured as stated previously[48, 49]. Briefly, equal number of cells were seeded per well in 96 well plates. After 72 hours treatment of indicated drugs or DMSO control 10 µl of MTS was added. After one hour incubation at 37 °C, absorbance was measured at 450 nm using a Tecan multi-well plate reader and data was represented as % viability compared to DMSO treated control as stated previously.

3.3.4 Proliferation and colony formation assays

Cell proliferation was measured as stated previously [44, 50]. Briefly, GBM6 cells were seeded in a 96 well plate at 3,000 cells per well in GBM media and cells were allowed to attach and enter log phase before drug treatment. DMSO, 2.9 µM (**5c**) and 3.3 µM (**5h**) were added. Every 24 hours afterwards, cell viability was assessed using CellTiter 96® AQueous One Solution Cell Proliferation Assay (MTS) kit following manufacturer's instructions and data was represented as % viability compared to DMSO treated control for a total of 5days.

For colony formation assay, approximately 500 cells/well of GBM143 were seeded onto a six- well plate. After overnight incubation cells were treated with **5c** or Temozolomide (TMZ) at 3 µM and 50 µM concentrations respectively. The control wells were treated with DMSO. Media was replaced every 3 days along with drug treatment. After 15 days colonies were fixed with methanol and stained using crystal violet (0.5% w/v in deionized water).

3.3.5 Spheroid invasion assay

3D spheroid invasion assay was carried out as stated previously[51]. Briefly, 2,000 GBM6 cells were seeded per well in a low attachment u-bottom 96 well plate (Thermo #174925) and spheroids were allowed to form over four days. These spheroids were embedded in Geltrex (Thermo #A1413302) which is a basement membrane extract that contains laminin, collagen IV, entactin, and heparin sulphate proteoglycans. The embedded spheroids were supplemented with complete media at top with or without drugs. The photomicrographs of each well containing

spheroid were taken at x100 resolution starting from day 0 (day of embedding the spheroid in matrix) through day 4 or day 6. The relative invasion was calculated using Image J software.

3.3.6 Cell cycle analyses

Cell cycle analyses using propidium iodide and flow cytometry were carried out as described previously[46, 50]. Asynchronous GBM6 cells were treated with either DMSO or **5c** at 3 µM for 16 hr. Post treatment, cells were washed with PBS+1% FBS and resuspended in flow cytometry tubes. Cells were then fixed with 70% ice-cold ethanol and propidium iodide (50 µg/ml) was added to the cells and incubated in the dark at room temperature (25°C) for 30 min. The cell populations were then subjected to quantitative measurement of DNA content by flow cytometry using a FACSFortessa (BD Biosciences) and cell cycle distribution and the percentage of G_2/M–S–G_1 cells to the total cell events were determined by the BD FACS Diva software. Stacked bar graphs were derived using Graphpad Prism.

3.3.7 Statistical Analysis

All statistical analysis was done using GraphPad Prism statistical package and presented as mean ± SD unless otherwise stated. Figure legends contain details of the statistical tests and multiple comparisons conducted throughout. Experiments were repeated 2-3 times with multiple technical replicates for the appropriate statistical tests to be conducted.

4. Conclusion

A series of bioactive novel alkoxy-functionalised DHPQ derivatives were synthesized using a multicomponent microwave-assisted reaction scheme employing glacial acetic acid. Out of the library we identified **5c** with the most potent anti-cancer activity in a diverse set of primary patient-derived glioblastoma cells. Furthermore, **5c** induced potent cytotoxicity, cell cycle anomalies, and anti-proliferative activity through ablation of key signalling pathway like JAK-STAT, MAPK, and AKT pathways. In fact, **5c** is more potent than glioma clinical drug temozolomide in killing GBM143 cells. Therefore, this study establishes a simple yet novel synthetic scheme which will allow for the development of future clinically relevant anti-cancer molecules which can be used to targeting diverse cancer growth pathways. Collectively, our data establishes **5c** as the most potent anti-cancer compound from the novel methoxy-DHPQ series of compounds tested. Further study is required as a future medicinal drugs.

Acknowledgements

Conflict of interest

The authors declare no conflict of interest.

References

1. Katzke, V. A.; Kaaks, R.; Kühn, T., Lifestyle and Cancer Risk. *The Cancer Journal* **2015,** *21* (2).
2. Nussbaumer, S.; Bonnabry, P.; Veuthey, J.-L.; Fleury-Souverain, S., Analysis of anticancer drugs: A review. *Talanta* **2011,** *85* (5), 2265-2289.
3. Stupp, R.; Mason, W. P.; van den Bent, M. J.; Weller, M.; Fisher, B.; Taphoorn, M. J. B.; Belanger, K.; Brandes, A. A.; Marosi, C.; Bogdahn, U.; Curschmann, J.; Janzer, R. C.; Ludwin, S. K.; Gorlia, T.; Allgeier, A.; Lacombe, D.; Cairncross, J. G.; Eisenhauer, E.; Mirimanoff, R. O., Radiotherapy plus Concomitant and Adjuvant Temozolomide for Glioblastoma. *New England Journal of Medicine* **2005,** *352* (10), 987-996.
4. Loch-Neckel, G.; Bicca, M. A.; Leal, P. C.; Mascarello, A.; Siqueira, J. M.; Calixto, J. B., In vitro and in vivo anti-glioma activity of a chalcone-quinoxaline hybrid. *European Journal of Medicinal Chemistry* **2015,** *90*, 93-100.
5. Nicely, L. G.; Baxter, M.; Banerjee, S.; Lord, H., Sacral ependymoma presents 20 years after initial posterior fossa lesion. *BMJ Case Reports* **2023,** *16* (10), e256611.
6. Keenlyside, A.; Marples, T.; Gao, Z.; Hu, H.; Nicely, L. G.; Nogales, J.; Li, H.; Landgraf, L.; Solth, A.; Melzer, A.; Hossain-Ibrahim, K.; Huang, Z.; Banerjee, S.; Joseph, J., Development and optimisation of in vitro sonodynamic therapy for glioblastoma. *Scientific Reports* **2023,** *13* (1), 20215.
7. Vala, R. M.; Tandon, V.; Nicely, L. G.; Guo, L.; Gu, Y.; Banerjee, S.; Patel, H. M., Synthesis of N-(4-chlorophenyl) substituted pyrano[2,3-c]pyrazoles enabling PKBβ/AKT2 inhibitory and in vitro anti-glioma activity. *Ann Med* **2022,** *54* (1), 2549-2561.
8. Bhalodiya, S. S.; Parmar, M. P.; Upadhyay, D. B.; Patel, C. D.; Vala, D. P.; Rajani, D.; Patel, H. M., Cs2CO3-promoted one-pot synthesis of novel tetrahydrobenzofuran-4 (2H)-ones: In vitro antimicrobial, antimalarial activity and in silico docking study. *Results in Chemistry* **2024,** *7*, 101304.
9. Patel, S. G.; González-Bakker, A.; Vala, R. M.; Patel, P. J.; Puerta, A.; Malik, A.; Sharma, R. K.; Padrón, J. M.; Patel, H. M., Microwave-assisted multicomponent synthesis of antiproliferative 2, 4-dimethoxy-tetrahydropyrimido [4, 5-b] quinolin-6 (7 H)-ones. *RSC advances* **2022,** *12* (47), 30404-30415.
10. Patel, S. G.; Patel, P. J.; Upadhyay, D. B.; Puerta, A.; Malik, A.; Kandukuri, N. K.; Sharma, R. K.; Padrón, J. M.; Patel, H. M., Insights into microwave assisted synthesis of spiro-chromeno[2,3-d]pyrimidines using PEG-OSO3H catalyst: DFT study and their antiproliferative activity. *Journal of Molecular Structure* **2023,** *1292*, 136174.
11. Wall, M. E.; Wani, M. C.; Cook, C. a.; Palmer, K. H.; McPhail, A. T. a.; Sim, G. A., Plant antitumor agents. I. The isolation and structure of camptothecin, a novel alkaloidal leukemia

and tumor inhibitor from camptotheca acuminata1, 2. *Journal of the American Chemical Society* **1966,** *88* (16), 3888-3890.

12.   Afzal, O.; Kumar, S.; Haider, M. R.; Ali, M. R.; Kumar, R.; Jaggi, M.; Bawa, S., A review on anticancer potential of bioactive heterocycle quinoline. *European journal of medicinal chemistry* **2015,** *97*, 871-910.

13.   Jain, S.; Chandra, V.; Jain, P. K.; Pathak, K.; Pathak, D.; Vaidya, A., Comprehensive review on current developments of quinoline-based anticancer agents. *Arabian Journal of Chemistry* **2019,** *12* (8), 4920-4946.

14.   Köprülü, T. K.; Ökten, S.; Atalay, V. E.; Tekin, Ş.; Çakmak, O., Biological activity and molecular docking studies of some new quinolines as potent anticancer agents. *Medical Oncology* **2021,** *38* (7), 84.

15.   Mao, Y.; Soni, K.; Sangani, C.; Yao, Y., An overview of privileged scaffold: quinolines and isoquinolines in medicinal chemistry as anticancer agents. *Current Topics in Medicinal Chemistry* **2020,** *20* (28), 2599-2633.

16.   Ghorab, M. M.; Ragab, F. A.; Heiba, H. I.; Arafa, R. K.; El-Hossary, E. M., In vitro anticancer screening and radiosensitizing evaluation of some new quinolines and pyrimido [4, 5-b] quinolines bearing a sulfonamide moiety. *European journal of medicinal chemistry* **2010,** *45* (9), 3677-3684.

17.   Ibrahim, N. S. M.; Kadry, H. H.; Zaher, A. F.; Mohamed, K. O., Synthesis of novel pyrimido [4, 5-b] quinolines as potential anticancer agents and HER2 inhibitors. *Chemical Biology & Drug Design* **2023,** *102* (5), 996-1013.

18.   El-Gamal, K. M., Synthesis and anticancer screening of heterocyclic compounds bearing pyrimido [4, 5-B] quinoline moiety. *International Journal of Pharmaceutical Sciences and Research* **2017,** *8* (2), 570.

19.   El-Ashmawy, M. B.; El-Sherbeny, M. A.; El-Gohary, N. S., Synthesis and antitumor screening of new series of pyrimido-[4, 5-b] quinolines and [1, 2, 4] triazolo [2′, 3′: 3, 4] pyrimido [6, 5-b] quinolines. *Medicinal Chemistry Research* **2013,** *22*, 2724-2736.

20.   Mohamed, M. F.; Abdelmoniem, A. M.; Elwahy, A. H. M.; Abdelhamid, I. A., DNA fragmentation, cell cycle arrest, and docking study of novel bis spiro-cyclic 2-oxindole of pyrimido [4, 5-b] quinoline-4, 6-dione derivatives against breast carcinoma. *Current Cancer Drug Targets* **2018,** *18* (4), 372-381.

21.   Ibrahim, N. S. M.; Kadry, H. H.; Zaher, A. F.; Mohamed, K. O., Synthesis of novel pyrimido [4, 5-b] quinoline derivatives as dual EGFR/HER2 inhibitors as anticancer agents. *Archiv der Pharmazie* **2023**, e2300513.

22.   Abu-Hashem, A. A.; Aly, A. S., Synthesis of new pyrazole, triazole, and thiazolidine-pyrimido [4, 5-b] quinoline derivatives with potential antitumor activity. *Archives of pharmacal research* **2012,** *35*, 437-445.

23.   El-Gohary, N. J. M. C. R., MB El-Ashmawy, MA El-Sherbeny &. **2013,** *22*, 2724-2736.

24.   Tieger, E.; Kiss, V.; Pokol, G.; Finta, Z.; Rohlíček, J.; Skořepová, E.; Dušek, M., Rationalization of the formation and stability of bosutinib solvated forms. *CrystEngComm* **2016,** *18* (48), 9260-9274.

25.   Bedi, S.; Khan, S. A.; AbuKhader, M. M.; Alam, P.; Siddiqui, N. A.; Husain, A., A comprehensive review on Brigatinib–A wonder drug for targeted cancer therapy in non-small cell lung cancer. *Saudi Pharmaceutical Journal* **2018,** *26* (6), 755-763.

26.	Wan, J.; Qiao, Y.; Chen, X.; Wu, J.; Zhou, L.; Zhang, J.; Fang, S.; Wang, H., Structure-guided engineering of cytotoxic cabazitaxel for an adaptive nanoparticle formulation: Enhancing the drug safety and therapeutic efficacy. *Advanced Functional Materials* **2018,** *28* (52), 1804229.

27.	Montazeri, K.; Bellmunt, J., Erdafitinib for the treatment of metastatic bladder cancer. *Expert Review of Clinical Pharmacology* **2020,** *13* (1), 1-6.

28.	Markham, A., Lurbinectedin: first approval. *Drugs* **2020,** *80*, 1345-1353.

29.	Larsen, A. K.; Galmarini, C. M.; D'Incalci, M., Unique features of trabectedin mechanism of action. *Cancer chemotherapy and pharmacology* **2016,** *77*, 663-671.

30.	Wang, H. L.; Andrews, K.; Booker, S. K.; Canon, J.; Cee, V. J.; Chavez, F., Jr.; Chen, Y.; Eastwood, H.; Guerrero, N.; Herberich, B.; Hickman, D.; Lanman, B. A.; Laszlo Iii, J.; Lee, M. R.; Lipford, J. R.; Mattson, B.; Mohr, C.; Nguyen, Y.; Norman, M. H.; Pettus, L. H.; Powers, D.; Reed, A. B.; Rex, K.; Sastri, C.; Tamayo, N. A.; Wang, P.; Winston, J. T.; Wu, B.; Wu, Q.; Wu, T.; Wurz, R. P.; Xu, Y.; Zhou, Y.; Tasker, A. S., Discovery of (R)-8-(6-Methyl-4-oxo-1,4,5,6-tetrahydropyrrolo[3,4-b]pyrrol-2-yl)-3-(1-methylcyc lopropyl)-2-((1-methylcyclopropyl)amino)quinazolin-4(3H)-one, a Potent and Selective Pim- 1/2 Kinase Inhibitor for Hematological Malignancies. *J Med Chem* **2019**.

31.	Asadi, B.; Mohammadpoor-Baltork, I.; Tangestaninejad, S.; Moghadam, M.; Mirkhani, V.; Landarani-Isfahani, A., Synthesis and characterization of Bi (III) immobilized on triazine dendrimer-stabilized magnetic nanoparticles: A reusable catalyst for the synthesis of aminonaphthoquinones and bis-aminonaphthoquinones. *New Journal of Chemistry* **2016,** *40* (7), 6171-6184.

32.	Dabiri, M.; Tisseh, Z. N.; Bazgir, A., Synthesis of fluorescent hydroxyl naphthalene-1, 4-dione derivatives by a three-component reaction in water. *Dyes and Pigments* **2011,** *89* (1), 63-69.

33.	Golmakaniyoon, S.; Askari, V. R.; Abnous, K.; Zarghi, A.; Ghodsi, R., Synthesis, characterization and in-vitro evaluation of novel naphthoquinone derivatives and related imines: Identification of new anticancer leads. *Iranian Journal of Pharmaceutical Research: IJPR* **2019,** *18* (1), 16.

34.	Shaabani, S.; Naimi-Jamal, M. R.; Maleki, A., Synthesis of 2-hydroxy-1, 4-naphthoquinone derivatives via a three-component reaction catalyzed by nanoporous MCM-41. *Dyes and Pigments* **2015,** *122*, 46-49.

35.	Jayashree, S.; Shivashankar, K., Montmorillonite K-10 catalyzed Mannich reaction: Synthesis of aminonaphthoquinone derivatives from Lawsone. *Synthetic Communications* **2018,** *48* (14), 1805-1815.

36.	Mollazehi, F., Comparison of nano catalysts in synthesis of hydroxyl naphthalene-1, 4-dione derivatives. **2019**.

37.	Paengsri, W.; Lee, V. S.; Chong, W. L.; Wahab, H. A.; Baramee, A., Synthesis, antituberculosis activity and molecular docking studies for novel naphthoquinone derivatives. **2012**.

38.	Patel, S. G.; Vala, R. M.; Patel, P. J.; Upadhyay, D. B.; Ramkumar, V.; Gardas, R. L.; Patel, H. M., Synthesis, crystal structure and in silico studies of novel 2, 4-dimethoxy-tetrahydropyrimido [4, 5-b] quinolin-6 (7 H)-ones. *RSC advances* **2022,** *12* (29), 18806-18820.

39.	Upadhyay, D. B.; Vala, R. M.; Patel, S. G.; Patel, P. J.; Chi, C.; Patel, H. M., Water mediated TBAB catalyzed synthesis of spiro-indoline-pyrano [3, 2-c] quinolines as α-amylase inhibitor and in silico studies. *Journal of Molecular Structure* **2023,** *1273*, 134305.

40.   Patel, P. J.; Patel, D. M.; Vala, R. M.; Patel, S. G.; Upadhyay, D. B.; Pannerselvam, Y.; Patel, H. M., Catalyst-Free, Room-Temperature Accessible Regioselective Synthesis of Spiroquinolines and Their Antioxidant Study. *ACS omega* **2022,** *8* (1), 444-456.

41.   Patel, P. J.; Vala, R. M.; Patel, S. G.; Upadhyay, D. B.; Rajani, D. P.; Damiri, F.; Berrada, M.; Patel, H. M., Catalyst-free synthesis of imidazo [5, 1-b] quinazolines and their antimicrobial activity. *Journal of Molecular Structure* **2023,** *1285*, 135467.

42.   Patel, P. J.; Patel, S. G.; Upadhyay, D. B.; Ravi, L.; Dhanasekaran, A.; Patel, H. M., An efficient, catalyst-free and aqueous ethanol-mediated synthesis of 5-((2-aminothiazol-5-yl)(phenyl) methyl)-6-hydroxypyrimidine-2, 4 (1 H, 3 H)-dione derivatives and their antioxidant activity. *RSC advances* **2023,** *13* (35), 24466-24473.

43.   Upadhyay, D. B.; Mokariya, J. A.; Patel, P. J.; Patel, S. G.; Das, A.; Nandi, A.; Nogales, J.; More, N.; Kumar, A.; Rajani, D. P., Indole clubbed 2, 4-thiazolidinedione linked 1, 2, 3-triazole as a potent antimalarial and antibacterial agent against drug-resistant strain and molecular modeling studies. *Archiv der Pharmazie* **2024**, e2300673.

44.   Banerjee, S.; Ji, C.; Mayfield, J. E.; Goel, A.; Xiao, J.; Dixon, J. E.; Guo, X., Ancient drug curcumin impedes 26S proteasome activity by direct inhibition of dual-specificity tyrosine-regulated kinase 2. *Proc Natl Acad Sci U S A* **2018,** *115* (32), 8155-8160.

45.   Banerjee, S.; Buhrlage, S. J.; Huang, H.-T.; Deng, X.; Zhou, W.; Wang, J.; Traynor, R.; Prescott, A. R.; Alessi, D. R.; Gray, N. S., Characterization of WZ4003 and HTH-01-015 as selective inhibitors of the LKB1-tumour-suppressor-activated NUAK kinases. *Biochemical Journal* **2014,** *457*, 215-225.

46.   Banerjee, S.; Zagorska, A.; Deak, M.; Campbell, D. G.; Prescott, A. R.; Alessi, D. R., Interplay between Polo kinase, LKB1-activated NUAK1 kinase, PP1 beta(MYPT1) phosphatase complex and the SCF beta TrCP E3 ubiquitin ligase. *Biochemical Journal* **2014,** *461*, 233-245.

47.   Nicely, L. G.; Vala, R. M.; Upadhyay, D. B.; Nogales, J.; Chi, C.; Banerjee, S.; Patel, H. M., One-pot two-step catalytic synthesis of 6-amino-2-pyridone-3,5-dicarbonitriles enabling anti-cancer bioactivity. *RSC Adv* **2022,** *12* (37), 23889-23897.

48.   Tandon, V.; Moreno, R.; Allmeroth, K.; Quinn, J.; Wiley, S. E.; Nicely, L. G.; Denzel, M. S.; Edwards, J.; de la Vega, L.; Banerjee, S., Dual inhibition of HSF1 and DYRK2 impedes cancer progression. *Biosci Rep* **2023,** *43* (1).

49.   Tandon, V.; Vala, Ruturajsinh M.; Chen, A.; Sah, Robert L.; Patel, Hitendra M.; Pirrung, Michael C.; Banerjee, S., Syrbactin-class dual constitutive- and immuno-proteasome inhibitor TIR-199 impedes myeloma-mediated bone degeneration in vivo. *Bioscience Reports* **2022,** *42* (2), BSR20212721.

50.   Banerjee, S.; Wei, T.; Wang, J.; Lee, J. J.; Gutierrez, H. L.; Chapman, O.; Wiley, S. E.; Mayfield, J. E.; Tandon, V.; Juarez, E. F.; Chavez, L.; Liang, R.; Sah, R. L.; Costello, C.; Mesirov, J. P.; de la Vega, L.; Cooper, K. L.; Dixon, J. E.; Xiao, J.; Lei, X., Inhibition of dual-specificity tyrosine phosphorylation-regulated kinase 2 perturbs 26S proteasome-addicted neoplastic progression. *Proc Natl Acad Sci U S A* **2019,** *116* (49), 24881-24891.

51.   Sharma, I.; Singh, A.; Siraj, F.; Saxena, S., IL-8/CXCR1/2 signalling promotes tumor cell proliferation, invasion and vascular mimicry in glioblastoma. *Journal of Biomedical Science* **2018,** *25* (1), 62.